# 30-cm Electron Cyclotron Plasma Generator

Hank Goede*
*TRW Space and Technology Group, Redondo Beach, California*

**Experimental results on the development of a 30-cm-diam electron cyclotron resonance plasma generator are presented. This plasma source utilizes samarium-cobalt magnets and microwave power at a frequency of 4.9 GHz to produce a uniform plasma with densities of up to $3\times10^{11}/cm^3$ in a continuous fashion. The plasma generator contains no internal structures, and is thus inherently simple in construction and operation and inherently durable. The generator was operated with two different magnetic geometries. One used the rare-Earth magnets arranged in an axial line cusp configuration, which directly showed plasma production taking place near the walls of the generator where the electron temperature was highest but with the plasma density peaking in the central low B-field regions. The second configuration had magnets arranged to form azimuthal line cusps with approximately closed electron drift surfaces; this configuration showed an improved electrical efficiency of about 135 eV/ion. Attempts were made to produce an overdense plasma—one in which the plasma frequency is greater than the microwave frequency—but these were not successful.**

## Nomenclature

$A_{it}$ = ion loss area, $cm^2$
$B$ = magnetic induction, G
$C$ = coulomb
$e$ = electronic charge, $1.6\times10^{-19}$ C
$L_B$ = magnetic field gradient scale length, cm
$m$ = mass of electron, $9.1\times10^{-31}$ kg
$T_e$ = electron temperature, eV
$V_{pp}$ = plasma production volume, $cm^3$
$v_{\nabla B}$ = electron drift velocity in a gradient magnetic field, cm/s
$\nu_c$ = electron ionizing collision frequency, $s^{-1}$
$\omega_{pe}$ = plasma frequency, $s^{-1}$
$\omega_\mu$ = microwave frequency, $s^{-1}$

## I. Introduction

ELECTRON cyclotron heating (ECH) at microwave frequencies typically between 2 and 30 GHz has been employed for many years for the production and heating of plasmas primarily for fusion applications.[1,2] Only occasionally has ECH been used for the production of inert gas plasmas for propulsion applications.[3,4] Some experimental results on the development of an ECH plasma source intended for 30-cm-diam primary electrostatic propulsion applications are presented.

Two of the goals of this undertaking were to develop a plasma source that was durable, in the sense of having the capability of operating unmaintained for many thousands of hours, and that possessed the feature of high electrical efficiency or low electron volts per ion. Limitations on the operational lifetime and stability of plasma sources can, in many cases, result from the hot, electron-emitting cathode structures that are directly immersed in the plasma and are thus subjected to direct ion bombardment. The production of a plasma in a source box, of course, requires the presence of energetic electrons that can ionize a gas and thus produce a discharge. However, these energetic ionizing electrons need not be born from a hot cathode situated in the plasma source, but can just as well be produced by judiciously coupled electromagnetic fields. For the case of an ECH plasma generator, the electromagnetic fields are produced by an oscillatory, such as a magnetron or a klystron, which, because these are high-vacuum tube devices, can operate for long time periods. The power required to produce and maintain the discharge is transmitted from the oscillator by coaxial line or waveguide and introduced by a simple coupling structure to the plasma source which is void of any critical components.

Previous ECH plasma sources for propulsion applications utilized a solenoidal volume magnetic field, produced by a relatively large electromagnetic, and accelerated ions by energy transferred through space-charge fields from the microwave-heated electrons without using any physical accelerating structure.[3,4] One of the problems encountered in these experiments was the survival of the microwave vacuum window, which, as a result of the geometry used, was subjected to intense, direct ion bombardment. The ECH plasma source to be described here avoids this problem through a change in geometry and by the utilization of magnetic fields produced by permanent magnets to keep the plasma away from the vacuum window.

The plasma generator described here uses samarium-cobalt magnets arranged in a multicusp,[5,6] surface-magnet-field geometry to provide the required 1.7-kG mod-B surfaces for resonant heatings at the applied frequency of 4.9 GHz. This operating frequency was chosen to provide a required total beam current of about 2 A of argon ions from the 30-cm-diam extraction plane. The maximum plasma density that could be obtained with this source was shown to be limited by the condition $\omega_{pe}<\omega_\mu$, where $\omega_{pe}$ is the plasma frequency and $\omega_\mu$ the radian frequency of the applied microwave power. The best efficiency achieved thus far was 185 eV/ion, obtained with an azimuthal-cusp magnetic geometry, which is one of the two magnetic variations described in the results of Sec. IV. The principle of operation and the experimental arrangement will be described in Secs. II and III, respectively. Concluding remarks are given in Sec. V.

Received April 1, 1986; revision received Sept. 2, 1986. 

*Staff Scientist, Applied Technology Division.

## II. Principle of Operation

A typical magnetic field geometry for ECH applications is the magnetic mirror geometry shown in Fig. 1. Here microwaves generally with wavelengths much less than the vacuum vessel dimensions are launched by simple antennas into the chamber which serves as an overmoded, high-$Q$ cavity. The microwave frequency $\omega_\mu$ is chosen to match the local electron cyclotron frequency, $\omega_{ce} = -eB/m_e$, on some surface between the mirror throat (the maximum B-field strength) and the midplane (the minimum B-field region). Electrons that pass through this resonance surface, which is very narrow in the direction along B, are heated by the local microwave electric fields. These energetic electrons, whose guiding centers are constrained to move along the flux lines, make ionizing collisions with the background neutral gas, and can thus create a plasma over the entire volume composed of those flux lines that intercept the resonant heating surface. By virtue of invariance of their magnetic moment, charged particles are confined by the magnetic trap of the mirror field and, as a consequence, a plasma discharge is easily initiated in this mirror geometry, even at very low microwave power levels and at very low ($<10^{-5}$ Torr) background neutral gas pressures.

Once a plasma has been produced, one must be concerned with the ability of the microwaves to propagate through the plasma and reach the resonant heating surface in order to sustain the discharge. For the special case in which the electromagnetic wave vector is purely perpendicular to the plasma-filled magnetic field lines, two principle modes of propagation can be identified. These are the ordinary (o) mode, with the electric field parallel to the magnetic flux line and the extraordinary (e) mode with the wave electric field perpendicular to the external B-field. The propagation characteristics for the e and o modes are shown schematically in Fig. 2 as a function of magnetic field strength ($\omega_{ce}/\omega_\mu$) and plasma density ($\omega_{pe}^2/\omega_\mu^2 = 4\Pi ne^2/(m\omega_\mu^2)$). Waves may be launched from either the high ($\omega_{ce} > \omega_\mu$) or low ($\omega_{ce} < \omega_\mu$) field side, and are required to reach the $\omega_{ce}/\omega_\mu = 1$ surface in order to resonantly heat electrons. While only the e mode is strongly absorbed in the neighborhood of the ECH zone, it has a cutoff when launched from the low field side. On the other hand, the o mode reaches the electron resonance zone from either the high or low field side, but becomes nonpropagating for plasma densities greater than $\omega_{pe}^2 > \omega_\mu^2$. This latter condition places a criterion on the maximum plasma density that can be obtained at a given microwave frequency, irrespective of the amount of power that is applied, when waves are launched from the low field side. The ordinary wave cutoff condition in turn limits the maximum ion current density that can be extracted from an ECH-based electrostatic thruster.

In many experiments, a mixture of ordinary and extraordinary waves is launched by the antenna, but very high absorption (>90%) is typically found. It has been shown[7] that the ordinary mode can undergo fairly strong partial conversion to the extraordinary mode upon reflection from the plasma-wall boundary. If the microwave Q of the plasma containment vessel is sufficiently high, all energy input in the ordinary mode will eventually be mode converted and absorbed.

ECH in conventional geometries is not suitable for current thruster technology, as superconducting magnets would be required to achieve the necessary field configuration without prohibitively high magnet power. The results described here utilize permanent magnets arranged in a multicusp configuration. Representative magnetic field lines and line of constant field strength for an infinite periodic multicusp array of long bar magnets are shown in Fig. 3.[8] Lines of constant B can be divided into two topological groups: those that intercept the magnets and those that do not. In considering a plasma in a periodic cusp field, two less distinct groups of field lines emerge. The field lines that remain in the high field region form a mirror-like configuration, while field lines extending into low field regions are associated with cusp-like plasma behavior.

In conventional multicusp sources, such as the multicusp hollow cathode discharges,[9] the source of ionizing electrons is in the low magnetic field region, i.e., on cusp-like field lines. For the ECH source described here, the frequency and permanent magnet field strength are such that the resonant heating surface is in the very high field strength region where most of

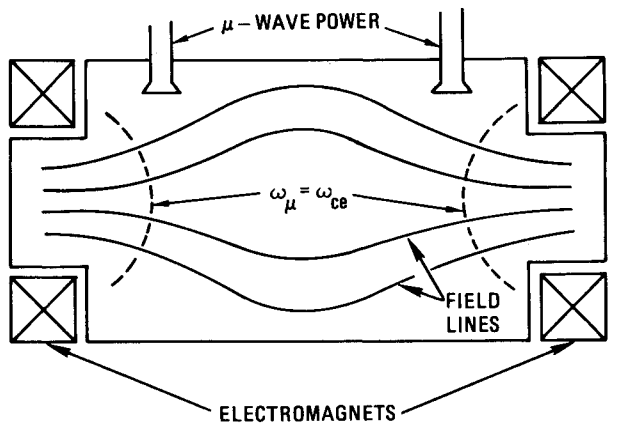


Fig. 1 Basic mirror geometry with ECH plasma production.

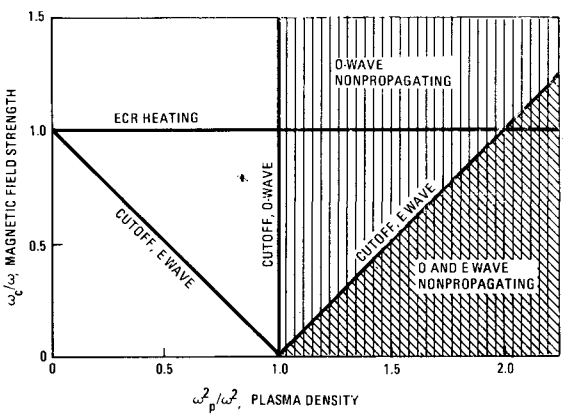


Fig. 2 Propagation and cutoff regions for ordinary and extraordinary modes for propagation perpendicular to a magnetic field.

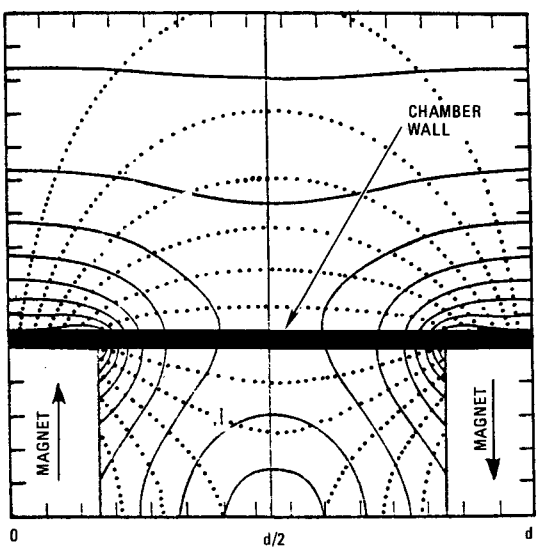


Fig. 3 Magnetic field lines (dotted) and lines of constant magnetic field (solid) for an infinite periodic array of bar magnets.

the magnetic field lines are mirror-like. Electrons are heated and confined to the mirror regions, quite contrary to conventional multicusp sources. Due to the magnetic field gradient and curvature, the plasma produced in the mirror-like regions of our ECH source is actually transported away from the source walls toward the weak field interior from which ions are extracted.

## III. Experimental Arrangement

The plasma generator housing used in these experiments was constructed of 1-mm-thick 304SS sheet rolled into a 30-cm-diam cylinder. One end of the cylinder was completely closed off by a disk of the same material to form the housing back plate. The purpose of using such thin material for the walls was to allow the placement of permanent magnets on the outside walls while maintaining the maximum possible B-field strengths near the housing interior surfaces. The other end of the cylinder was fitted with a 30-cm-diam, 5-mm-thick copper plate, which was uniformly perforated with 2.4-mm-diam holes to allow observation of the plasma as well as gas pumping. This copper disk, or termination plate, was electrically floated from the rest of the housing, and could, by proper biasing, simulate the ion extraction area that an actual 30-cm electrostatic grid set would present. The entire housing was placed within a larger vacuum chamber, into which argon gas was fed and pressure sensing was accomplished. As no cooling provisions were made for the housing, thermocouples were placed in contact with the source walls to monitor their temperature. Experiments were discontinued when the housing temperature reached about 200°C, as this was approximately the temperature at which the samarium-cobalt magnets could be irreversibly damaged. (200°C is considerably below the Curie temperature.) This allowed for up to 4h of continuous operation at 700-W input power levels.

All data on this ECH ion source was obtained with the use of a Varian (VA888) klystron amplifier tuned to an operating frequency of 4.9 GHz. The microwave circuit configuration is shown in Fig. 4. A low-level oscillator with variable attenuation output drives the amplifier. A high-power circulator is used to protect the amplifier from excessive reflected power, which can occur due to load impedance variations. Microwave power is transferred to the plasma generator chamber by fundamental mode, rectangular waveguide. A microwave vacuum window was mounted about 30 cm away from the source housing. Although commercial windows are available, we constructed our own using a design that incorporated a 1.6-mm-thick quartz window with dimensions 1.6 mm greater than the standard inside dimensions of the waveguide. This quartz plate was mounted with Torr Seal™ to a standard milled flange and had a measured VSWR of 1.4 at the operative frequency. This window has survived without failure for many tens of hours of operation at 1·kW power levels.

The plasma density, electron temperature, space potentials, and their spatial variations were all obtained from standard Langmuir probe traces. The Langmuir probe usually consisted of a 0.0229-cm-diam, 0.50-cm-long tungsten cylinder. Special care was taken in the construction of this probe, as the intense microwave fields that exist in the source chamber can destroy most insulating materials (such as glass weaving and aluminum oxide) and, at times, can cause the tungsten probe to glow white hot. Additional information on the extractable current density was obtained from the total ion current collected by the negatively biased, perforated copper termination plate.

## IV. Experimental Results

### Axial Line Cusp Configuration

The initial operation of the ECH source utilized 12 rows of uniformly spaced, alternating polarity $SMCo_5$ magnets mounted to the outside cylindrical walls of a 30-cm-long chamber, as sketched in Fig. 5. The multidipole line cusps

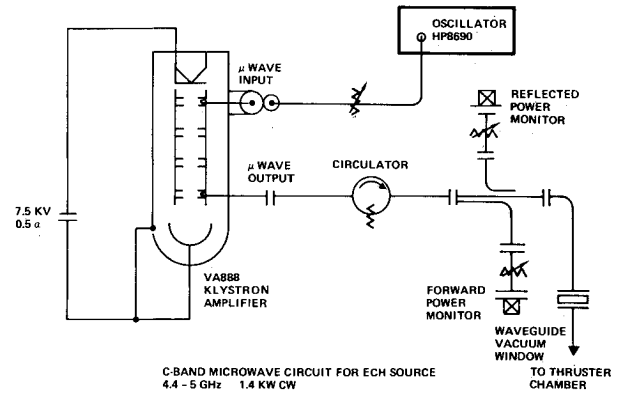


**Fig. 4 C-band microwave circuit for ECH source.**

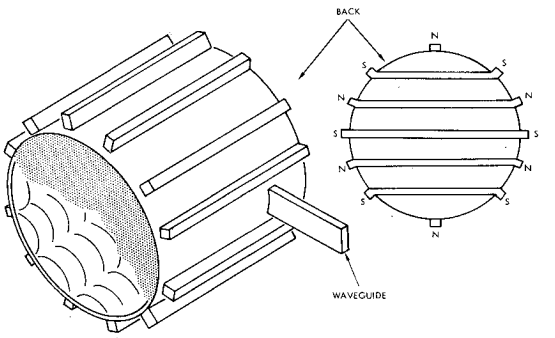


**Fig. 5 ECH source with the axial line cusp magnet configuration.**

were continued on the back plate with five rows of magnets. The magnet rows were assembled from magnets with dimensions $1.27\uparrow \times 1.27 \times 2.54$ cm and cubes of 1.27 cm. (↑ indicates the direction of magnetization.) These magnets were mounted on 0.318-cm-thick cold rolled steel strips to double their effective aspect ratio and produced measured pole face magnetic fields of about 4.5 kG. This ensured that the electron heating zone, which is $B = 1.75$ kG at $f_\mu = 4.9$ GHz, was about 0.5 cm from the inside surface of the housing.

The microwave feed configuration consisted of a standard C-band waveguide soldered to the perimeter of a hole cut out of the cylinder wall of the chamber. This feed and magnet arrangement is approximately such that an extraordinary mode is launched from the guide.

Although a startup electron source was initally included in the design, it proved to be unnecessary as the discharge was self-initiating at power levels above 75 W at argon neutral pressures above $1 \times 10^{-4}$ Torr. This easy startup is a result of the reasonably high Q of the chamber, which allows the microwave fields to build up to breakdown levels even at modest input powers.

Figure 6 is a photograph of the discharge at a microwave input power of 100 W. The bright regions of plasma at the periphery are zones of high electron energy where most of the plasma production occurs. As hypothesized, these zones are the mirror-like magnetic field regions where electrons are confined. Each of the bright regions appears to terminate at the very edges of the magnets, while the majority of the field lines emanating from the central portions of the magnet pole faces appear dark, indicating low electron temperature and little plasma production. Between adjacent magnets at the cylindrical walls, we note that the bright regions dip toward and touch the walls. This behavior, which should not occur if the electron guiding centers strictly follow the magnetic field lines, may be the result of an interchange or flute-like instability,[10] which occurs in regions where magnetic field lines have

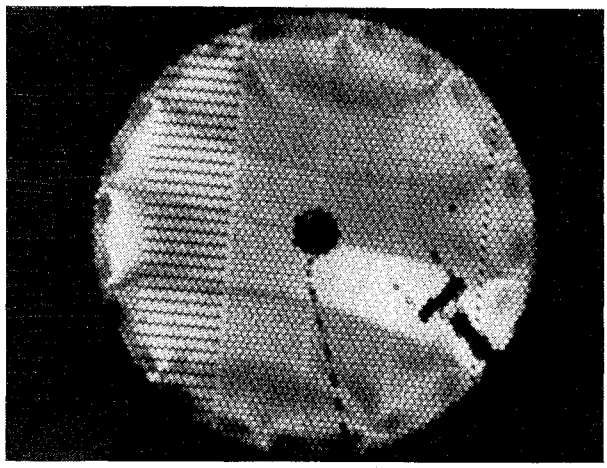

**Fig. 6 Front view of the ECH source. Bright regions are zones of plasma production.**

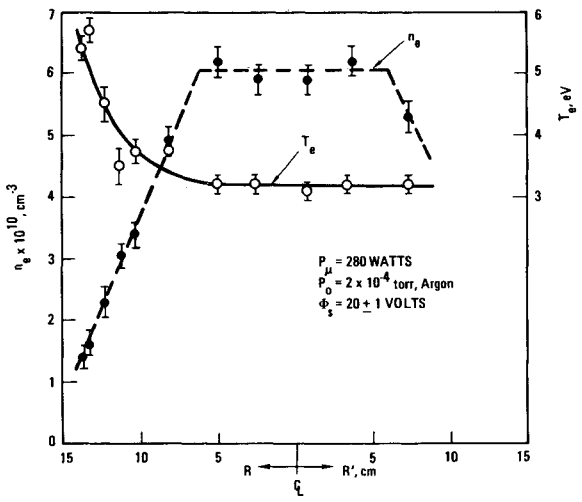


**Fig. 7 ECH source radial electron density and temperature profiles for the axial line cusp configuration.**

**Table 1 Grid current and eV/ion as a function of power and neutral pressure for the azimuthal geometry**

| $P_0 \times 10^{-4}$ Torr | $P_{\mu F}$, W | $P_{\mu R}$, W | $P_{\mu N}$, W | $I_G$, A | $P_{\mu N}/I_G$ |
|---|---|---|---|---|---|
| 1.6 | 200 | 22 | 178 | 0.4 | 445 |
| 1.6 | 290 | 154 | 136 | 0.8 | 170 |
| 1.6 | 400 | 70 | 330 | 1.55 | 213 |
| 1.6 | 500 | 62 | 438 | 1.7 | 258 |
| 1.6 | 605 | 126 | 479 | 1.8 | 266 |
| 1.6 | 710 | 214 | 496 | 1.8 | 276 |
| 2.4 | 240 | 19 | 221 | 0.95 | 232 |
| 2.4 | 320 | 41 | 279 | 1.5 | 186 |
| 2.4 | 410 | 69 | 341 | 1.55 | 220 |
| 2.4 | 535 | 126 | 409 | 1.9 | 215 |
| 2.4 | 600 | 120 | 480 | 2.4 | 200 |
| 2.4 | 700 | 164 | 536 | 2.6 | 206 |
| 3.6 | 220 | 19 | 201 | 0.9 | 223 |
| 3.6 | 380 | 38 | 342 | 2.0 | 171 |
| 3.6 | 520 | 114 | 406 | 2.5 | 162 |
| 3.6 | 620 | 151 | 469 | 2.8 | 168 |
| 3.6 | 730 | 183 | 547 | 3.0 | 182 |
| 4.8 | 230 | 25 | 205 | 1.2 | 171 |
| 4.8 | 300 | 35 | 265 | 1.25 | 212 |
| 4.8 | 420 | 100 | 320 | 2.4 | 133 |
| 4.8 | 500 | 164 | 336 | 2.5 | 134 |
| 4.8 | 615 | 252 | 363 | 2.5 | 145 |

average unfavorable curvature. This instability would clearly adversely affect particle confinement and reduce engine efficiency. One should also note that in Fig. 6 the bright regions on the back plate alternate from right to left. For example, the lowest strip of plasma at the back plate is brightest on the right side, while the next strip up is brightest on the left side of the chamber. This effect is due to the $\nabla B$ drift of electron guiding centers, which cause electrons to drift across the field lines and build up at the edges, resulting in bright regions.

Figure 7 shows the inverted radial temperature profile obtained from measurements with a Langmuir probe positioned 5 cm from the copper grid and centrally located between two magnet rows. The central portion of the discharge chamber contains Maxwellian electrons of temperature 3.1 eV. Near the periphery, where most of the plasma production occurs, the temperature reaches 6–7 eV. Probe measurements in the high magnetic field regions should be interpreted only as indicative of the temperature, as the probe considerably perturbs the plasma in this region. Nonperturbing optical measurements of line intensities of trace amounts of helium bled into the system have indicated that temperatures as high as 20 eV exist in this ECH source.

The plasma density profile, also illustrated in Fig. 7, is peaked in the central region of the chamber, indicating that the plasma is rapidly transported from the high magnetic field to the low field region. The plasma density does not peak where most of the production takes place. The plasma potential with respect to the generator walls was $20 \pm 1$ V positive independent of radial position. The floating potential (i.e., the probe voltage at which equal electron and ion currents are collected), on the other hand, was measured to be 4.5 V positive with respect to the wall in the central regions, and decreased, starting at $r = 10$ cm, to a negative 5 V near the thruster housing. The copper grid that simulates the extraction grids had a floating potential of positive 10 V with respect to the chamber walls, or negative 10 V with respect to the plasma, a result of the low electron temperature in the vicinity of the grid.

Although the discharge cavity was large enough that theoretically a particular discrete microwave mode should not be preferred (i.e., there should be mode overlap), the discharge did exhibit a number of discrete "modes," especially at applied microwave powers of less than 300 W. Some of the moding characteristics are illustrated in Fig. 8, which shows electron density and reflected microwave power as a function of applied microwave power. A particular discharge mode, which is characterized by breakdown in an isolated location of the chamber, forms at an applied power of 100 W with a plasma density in the central low B-field region of $1.5 \times 10^{10}$ cm$^{-3}$ and a reflected power of 20 W. As the applied power is increased up to a value of approximately 300 W, the plasma density remains unchanged, with the additional power merely being reflected back toward the microwave source. At the applied power of slightly greater than 300 W, the discharge jumped into a mode characterized by plasma production in all peripheral mirror regions. In this mode, the central density increased linearly with applied power.

The electron density and ion current to the copper grid as a function of net input power (applied minus reflected power) are illustrated in Fig. 9. The electron temperature in the central regions of the chamber was independent of applied power at fixed neutral pressure. The ion current collected by the 700-cm$^2$ grid biased at $-60$ V increased linearly with net input power and corresponds to discharge chamber losses of about 280 eV/ion, assuming all net power is absorbed by plasma electrons. The measured reflected power, in the region where the collected ion current is linearly proportional to applied power, represents about 30% of the forward power. In the low-power "mode," characterized by a very localized plasma production volume, the eV/ion (calculated from net power) is approximately 550–600 V. This suggests that the efficiency could be improved by an increase in the production volume perhaps through the use of microwave power at a lower frequency.

Another factor that can affect the source production efficiency is that none of the electron drift surfaces are closed in this axial line cusp geometry. Direct evidence of this was shown in Fig. 6. The electron guiding center drift, which is in the direction of $\bar{\nabla}B\times\bar{B}$, can cause electrons to be lost to the chamber walls before they have a chance to ionize neutral atoms. Assuming perfect mirror confinement of electrons confined to magnetic field lines that pass through the resonance zones, one would like these heated electrons to make at least one ionizing collision before being lost via $\bar{\nabla}\bar{B}$ drift to the walls. We, therefore, expect this drift to be important if spatial lengths of roughly

$$\ell\,(\text{cm}) \geq \frac{v_{\nabla B}}{\nu_c} = \frac{1}{\nu_c}\,\frac{T_e(\text{eV})}{B\,(\text{G})}\,\frac{1}{L_B\,(\text{cm})} \times 10^8 \qquad (1)$$

or greater are encountered in the generator. Here $\nu_c$ is the ionizing collision frequency, and $L_B$ is the magnetic field gradient scale length. Of course, if the $\bar{\nabla}B$ drift surfaces are closed and do not intercept the chamber walls or other obstacles, we would expect better energetic electron utilization and, hence, lower eV/ion values. The results of such a configuration are described subsequently.

### Azimuthal Line Cusp Configuration

The results described here utilized a magnet configuration with three line cusps of $SmCo_5$ arranged azimuthally about the 30-cm-diam cylindrical wall, as shown in Fig. 10. These magnet rings, which had pole face fields of 4.5 kG, were arranged with a center-to-center spacing of 5.5 cm. The downstream magnet ring was placed 2.0 cm from the copper collection plate, while the upstream ring was placed 2.0 cm from the edge where the back was attached. The discharge chamber length was thus 15 cm—half of the length of the configuration with axial line cusps. The back plate also had alternative polarity ring cusps mounted to it as shown. The central 5-cm-diam disk was samarium cobalt, with pole face fields equal to 3.0 kG, while the other two rings on the back plate were of ceramic material with pole face fields of 1.5 kG. This configuration has closed drift surfaces everywhere assuming error fields are negligible.

The microwave feed was again a standard C-band guide soldered to the back plate between the nonresonant ceramic magnet rings to help prevent breakdown directly in front of the feed. Note that in this configuration the feed is approximately such as to launch an ordinary mode wave.

The radial plasma density profile, taken with a probe 4 cm from the copper grid, is shown in Fig. 11. Comparison of this profile with the profile of Fig. 7, for the axial line configuration, shows that the azimuthal configuration is uniform over a larger extraction area. This will allow greater ion current to be drawn to the copper grid in the azimuthal configuration than in the axial line arrangement. Flatter profiles than indicated in Fig. 11 may presumably be obtained at the extraction grid by adjusting the axial position of the magnet ring closest to the grid. In theory, with a flatness parameter of 1, it should be possible to draw a total of 4.6 A of argon to the 700-$cm^2$ grid even when the plasma density in this ECH source is limited by the cutoff density of $3\times10^{11}$ $cm^{-2}$ for 4.9-GHz power and the electron temperature at the grid is only 3 eV. Therefore, we expect that, with proper design, one should be able to draw a 3-A beam from the source using a 65% transparent screen.

Note that the temperature profile also shown in Fig. 11 has the same inverted shape as the axial line cusp configuration, but does not appear to be as steep. The electron temperature in the central regions of the chamber was again about 3 eV—the same as in the axial configuration—but increases to only about 3.5 eV near the walls. The reason for this is that quite unexpectedly the majority of electron heating and plasma production appeared to be restricted to the back plate magnetic fields under conditions of high neutral pressure and high

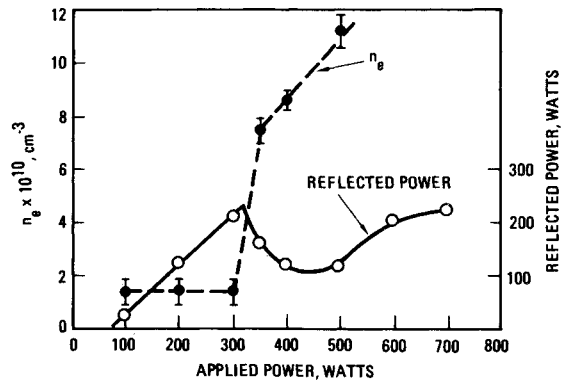


**Fig. 8 Plasma density in the central region of the ECH source as a function of the applied microwave power. Also indicated is the microwave power reflected back into the feed guide.**

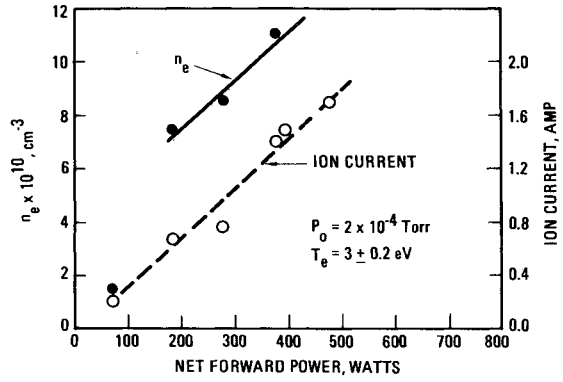


**Fig. 9 Plasma density and ion current collected by the grid as a function of total microwave power absorbed by the plasma electrons.**

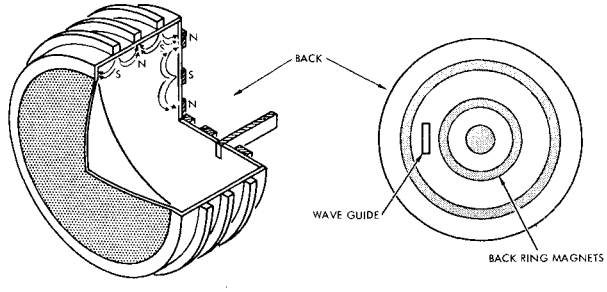


**Fig. 10 Magnet and power feed arrangement for the azimuthal cusp configuration.**

microwave power. Very little power appears to be coupled to electrons in the fields of the magnets at the cylindrical walls. If this is true, then it may be possible to eliminate the magnets on the cylindrical walls entirely and shorten the thruster to a length of 6–8 cm without causing a reduction in performance; in fact, the performance may improve over the eV/ion values stated in the following section because cylindrical wall losses would be largely reduced. Gas utilization would of course be reduced.

The electrical efficiency of this azimuthal line cusp configuration is summarized in Table 1. The ion current ($I_G$) collected by the copper grid, biased 35 V negative to the chamber housing, is given as a function of net power ($P_{\mu N}$) at various neutral pressures. The net power divided by the grid current gives the electron volts per nonextracted ion values. The general trend is that the eV/ion decreases as the neutral pressure increases. A minimum eV/ion of 135 was obtained.

**Table 2 Parameter comparison of a discharge terminated with a copper grid and one terminated with a wall of magnets. Argon gas pressure was fixed at $2\times10^{-4}$ Torr**

| $P_{\mu F}$, W | $P_{\mu R}$(Watt) | $P_{\mu N}$(Watt) | $n_e\times10^{10}$(cm$^{-3}$) | $T_e$(eV) | $n_e/P_{\mu N}\times10^8$ |
|---|---|---|---|---|---|
| | | Case 1—with grid (bias = −60 V) | | | |
| 100 | 16 | 84 | 1.4 | 3.1 | 1.6 |
| 200 | 79 | 121 | 1.45 | 3.1 | 1.2 |
| 300 | 132 | 168 | 1.35 | 3.2 | 0.8 |
| 350 | 100 | 250 | 7.4 | 3.0 | 3.0 |
| 400 | 76 | 324 | 8.5 | 3.0 | 2.6 |
| 500 | 76 | 424 | 11.0 | 2.8 | 2.6 |
| | | Case 2—without grid (magnets on all walls) | | | |
| 300 | 63 | 237 | 6.9 | 3.1 | 2.9 |
| 400 | 107 | 293 | 14.0 | 2.0 | 4.8 |
| 550 | 151 | 400 | 19.0 | 2.4 | 4.8 |
| 700 | 214 | 486 | 22.0 | 2.1 | 4.5 |
| 860 | 277 | 583 | 23.0 | 2.1 | 3.9 |

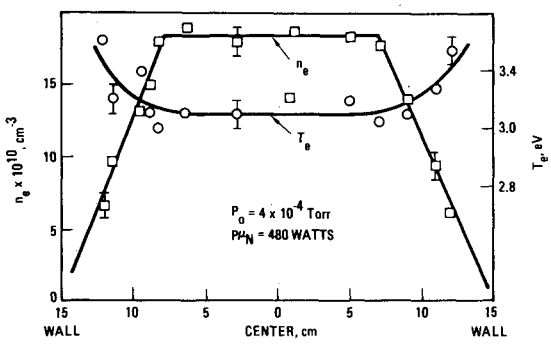


**Fig. 11 Radial profiles of plasma density and electron temperatures near the extraction grid in the azimuthal geometry.**

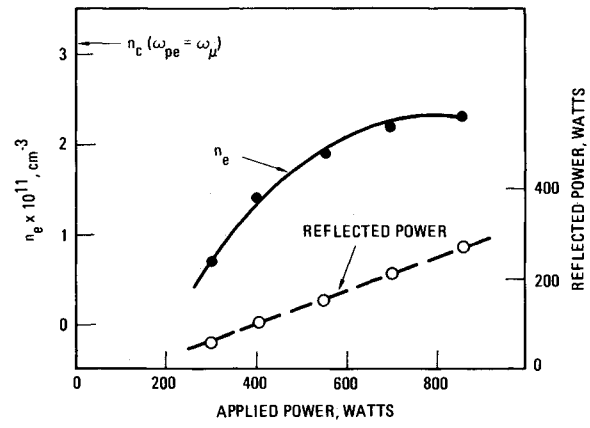


**Fig. 12 Central volume plasma density as a function of power in an attempt to achieve an overdense plasma.**

Whether this reduction by almost a factor of 2 for this azimuthal geometry ECH source as compared with the axial geometry ECH source is a result of closed drift surfaces has not yet been ascertained. It may be that the improved efficiency is simply a result of reducing the discharge volume by a factor of 2. Although these results are encouraging, it should be noted that a substantial fraction, 20–30, of the forward power is being reflected back down the feed guide under optimal extraction conditions. An E-H tuner installed on the high-pressure side of the microwave vacuum window was unable to reduce the quantity of reflected power substantially. We believe that a reduction in reflected power can be achieved by varying the relative geometry between the microwave feed and the magnetic configuration.

#### Attempt to Achieve an Overdense Plasma

Although this ECH plasma generator was designed to operate with an underdense plasma (i.e., $\omega_\mu > \omega_{pe}$), it would be advantageous to remove this requirement for at least the following reasons: First, higher-efficiency microwave sources are available at lower frequencies. Second, the use of lower microwave frequencies would allow greater freedom in magnet design by possibly reducing the magnet mass or by improving the thruster performance since heating surfaces could be moved further from the magnet pole faces.

Here, an attempt has been made to produce an overdense ($\omega_{pe} > \omega_\mu$) plasma using the magnet and microwave feed configuration shown in Fig. 5. The only change was to replace the copper grid with a plate identical to the back plate already attached to the housing. Therefore, with all chamber walls covered with magnetic line "cusps," the loss area would be reduced and the maximum achieved density would not be a consequence of microwave power limitations.

The measured plasma density in the central regions of the chamber as a function of applied power is shown in Fig. 12. The density saturates with increased power and asymptotically approaches a density that is about 75% of the cutoff density of the ordinary mode for 4.9 GHz. These Langmuir probe density measurements are estimated to be accurate to about ±20%. Since the measurements were made in the central volume of the chamber where the density has been shown to be a maximum, we conjecture that the density at the resonance zones near the magnet pole faces must be about the same as in the central volume. If this were not the case, it would be difficult to imagine why the density saturates very near the cutoff density. We had hoped that an overdense plasma might be achieved since the resonance zones are very near the low-density regions between magnet rows. As seen from Fig. 7, the density between the magnets and near the walls is about an order of magnitude lower than the density in the central region. The microwaves, therefore, would propagate in this underdense plasma until they reach the cutoff near the resonance zone. Since the collisionless skin depth $c/\omega_{pe}$ is roughly 1 cm for a $3\times10^{11}$ cm$^{-3}$ density plasma, the waves could penetrate with sufficient amplitude to maintain electron heating. However, it would appear from these results that this does not occur.

The reflected microwave power measurements shown in Fig. 12 do not increase sufficiently as the plasma density approaches saturation. At the cutoff density, the microwaves

should be totally reflected if the absorption mechanism, first mentioned, does not occur, as seems to be the case. Therefore, at the cutoff density, when the applied power is increased, the reflected power should increase by a corresponding amount. However, this does not occur.

Table 2 summarizes and compares the central volume density and electron temperature as a function of applied microwave power for the case when the chamber is terminated with the copper grid (case 1) and the case when the grid is replaced with a wall of line cusp magnets (case 2). With magnets on all walls, the electron temperature is lower, because the ratio of plasma production volume to ion loss area, $V_{pp}/A_{il}$, is larger for the case with magnets on all walls than for that with the grid termination. It is well known that devices with larger effective length, $L = V_{pp}/A_{il}$, can be expected to operate at lower electron temperatures at a given neutral gas pressure. The data in Table 2 also indicate that the plasma density per net watt of input power is approximately a factor of 2 higher with magnets on all walls. Since the fractional increase in production volume of case 2 over case 1 is too small to account for the factor of 2 increases in $n_e/P_{\mu N}$, it must be that the surface magnetic (or electric) fields do provide some ion confinement. However, systematic comparisons of different configurations with this ECH source for the purpose of examining ion confinement are difficult, in part due to the various plasma "modes" that exist. Such difficulty may be seen, for example, in Table 2 by comparing $n_e/P_{\mu N}$ values for $P_{\mu F} = 350$ and 300 W in cases 1 and 2, respectively Approximately the same net power is measured in each case and the values of $n_e/P_{\mu N}$ are nearly identical—a result that could be interpreted as showing that there is absolutely no ion confinement.

## V. Conclusion

The initial development of a plasma generator based on electron cyclotron heating that utilizes 4.9-GHz microwave power and magnetic fields of strength up to 4.5 kG is described. The source is designed to incorporate electrostatic acceleration through the use of physical grids to form the ion beam for useful purposes. The magnetic geometry is such that low residual magnetic fields of order 10 G are present at the extraction region; these fields should not influence the optical performance of an acceleration system based on magnetic field free theory.

The data obtained to date with this electron cyclotron heating (ECH) source validates the basic concept. Certain aspects of this source are particularly attractive.

Since the source is electrodeless, any lifetime problems associated with cathodes or antennas immersed in the plasma are eliminated. Ion losses to these structures are also absent. The ECH source plasma exhibits a very low Maxwellian electron temperature and, hence, low space potential in the vicinity of the extraction grid. This should lead to greatly reduced screen and discharge chamber sputter rates. The construction of the discharge chamber is quite simple, requiring only a metal housing and microwave feed connection.

The discharge chamber losses reported here have been reduced from best initial values of order 250 eV/ion to approximately 130 eV/ion for the azimuthal magnet configuration. The lower figure translates into about 185 eV/beam ion of the 70% transparency optical structure used for beam extraction.

There are some issues that should be addressed in any further development of this type of ECH plasma source. One should gain a better understanding of the plasma transport processes that occur. For example, how does the central volume of the source fill with high density when plasma production clearly takes place on magnetic field lines very close to the source walls. One would also like to be able to control the discrete plasma "modes" in which only a localized region appears to contain heated, ionizing electrons. While this "moding" did not occur at higher power levels (>300 W), it can have consquences when smooth, continuous control on the extractable ion current density is desired, as in engine throttling for electrostatic thruster applications.

In summary, this ECH plasma generator performed well in terms of electrical efficiency, reliability, and simplicity of operation. It provides a steady-state, uniform plasma density of $3 \times 10^{11}/\text{cm}^3$, limited by the frequency of the applied microwaves. This device contains no internal electrode structures or antenna and could thus be used not only for the production of inert gas plasmas, but also for production of plasmas of exotic materials.

## Acknowledgments

The author wishes to acknowledge his thanks for many enlightening and useful discussions on this work with W. F. DiVergilio. This work was supported by NASA Lewis Research Center under Contract NAS3-22473.

## References

[1]Dandl, R.A., England, A.C., Ard, W.B., Eason, H.O., Becker, M.C., and Haas, G.M., "Properties of a High-Beta Plasma Produced by Electron-Cyclotron Heating," *Nuclear Fusion,* Vol. 4, 1964, p. 344.

[2]Sprott, J.C., "Electron Cyclotron Heating in Toroidal Octupoles," *The Physics of Fluids,* Vol. 14, 1971, p. 1975.

[3]Miller, D.B., Bethke, G.W., and Crimi, G.F., "Investigations of Plasma Accelerator," NASA CR-54746, Nov. 1965.

[4]Kosmahl, H.G., Miller, D.B., and Bethke, G.W., "Plasma Acceleration with Microwaves Near Cyclotron Resonance," *Journal of Applied Physics,* Vol. 38, 1967, p. 4576–4582.

[5]Ramsey, W.D., "12-cm Magnetic-Electrostatic Containment Mercury Ion Thruster Development," *Journal of Spacecraft and Rockets,* Vol. 9, 1972, p. 318–321.

[6]Limpaecher, R. and MacKenzie, K., "Magnetic Multipole Containment of Large Uniform Collisionless Quiescent Plasmas," *Rev. Sci. Instr.,* Vol. 44, 1973, p. 726.

[7]Batchelor, D.B., Goldfinger, R.C., and Rasmussen, D.A., "Detailed Modeling of Microwave Energy Deposition in EBT Devices," *The Physics of Fluids,* Vol. 27, 1984, p. 948–961.

[8]Samec, T.K., "Plasma Confinement by Surface Magnetic Fields," Dissertation, University of California, Los Angeles, Department of Plasma Physics Report PPG-281, Nov. 1976.

[9]Kaufman, H.R., "Technology of Electron-Bombardment Ion Thrusters," *Advances in Electronics and Electron Physics,* Vol. 36, Academic, 1974, p. 345.

[10]Mikhailovski, A.B., *Theory of Plasma Instabilities,* Vol. 2, Consultants Bureau, New York, 1974, p. 113.